Received: 19 April 2016 | Revised: 12 July 2016 | Accepted: 26 July 2016

DOI 10.1002/poc.3629

WILEY Journal of Physical Organic Chemistry

RESEARCH ARTICLE

High diastereoselectivity induced by intermolecular hydrogen bonding in [3 + 2] cycloaddition reaction: experimental and computational mechanistic approaches

Ayhan Yıldırım[1]* | Yunus Kaya[2]

[1] Department of Chemistry, Uludağ University, 16059 Bursa, Turkey

[2] Department of Chemistry, Faculty of Natural Sciences, Architecture and Engineering, Bursa Technical University, Bursa, Turkey

Correspondence
Ayhan Yıldırım, Department of Chemistry, Uludağ University, 16059 Bursa, Turkey.
Email: yildirim@uludag.edu.tr

Abstract

A diastereoselective [3 + 2] cycloaddition of *N*-aryl substituted maleimides with *N*,*α*-diphenyl nitrone possessing 11-hydroxyundecyloxy as a flexible substituent was performed. Experimental and comprehensive mechanistic density functional theory studies reveals that intermolecular H-bonding and steric repulsive interaction predominate *exo-Z* and *exo-E* cycloaddition transition states, respectively. The reaction proceeded smoothly depending on the reactants and gave a good yield of (*syn*) *cis*-isoxazolidine or (*anti*) *trans*-isoxazolidine as a single diastereomer.

KEYWORDS

DFT, diastereoselective synthesis, H-bonding, maleimide, nitrone, transition states

1 | INTRODUCTION

Cycloaddition reactions between acyclic/cyclic nitrones (azomethine-*N*-oxides) and *N*-aryl substituted maleimides have been studied extensively in the last 2 decades.[1–14] As is well known aldonitrones may have 2 configurations that may interconvert. One of them is the *syn* or *E* configuration and the other is the *anti* or *Z* configuration. In some studies UV and nuclear magnetic resonance (NMR) spectroscopic analysis pointed out that the *Z* configuration is more preferred.[15]

A typical reaction between nitrone and *N*-substituted maleimide results in formation of fused 5 membered isoxazolidine cycloadduct. Generally, depending on the structure of the starting compounds, 2 diastereoisomers can occur, each with 2 enantiomers.[3,7,10–12]

Cycloaddition reactions between diarylnitrones and electron-deficient dipolarophiles may proceed via concerted or (alternatively) stepwise zwitterionic mechanism.[16,17]

In the literature, there are various examples of diastereoselective intramolecular and intermolecular [3 + 2] cycloaddition reactions.[18–24] O'Neil et al reported a highly diastereoselective intramolecular cycloaddition of cyclic nitrone obtained via *Cope elimination* to give tricyclic isoxazolidines.[18] Bakthadoss and Devaraj also reported diastereoselective intramolecular nitrone cycloaddition furnishing some tetrahydroquinolinoisoxazoles.[19] On the other hand, intramolecular reaction of nitrones derived from optically active aldehyde allows diastereoselective synthesis of some fused isoxazolidines.[20] Banerji et al isolated diastereomeric isoxazolidines from the intermolecular reaction between methyl cinnamate and nitrone with stereocontrol provided by different reaction conditions.[21] In addition, some studies presented that triflates can be used as a catalyst to provide diastereoselectivity in [3 + 2] cycloadditions.[22–24]

Merino et al[25] and Mekelleche and Benchouk[26] have reported studies that include computational investigation of diastereoselectivity in intermolecular reactions between nitrones-1,2-diaza-1,3-dienes and nitrone-methacrolein, respectively.

There are some studies on H-bonding–induced diastereoselectivity in different reactions.[27–30] Kilic et al reported that diastereoselectivity can be obtained through H-bonding in some aziridination reactions.[27] On the other hand, according to Jones et al[28] and Aviyente et al[29] diastereoselective [4 + 2] cycloadditions can also be performed guided by H-bonding. One study reported that internally H-bonded chiral methylene nitrones undergo diastereoselective [3 + 2] cycloaddition.[30] In addition several examples exist in the literature for H-bonding–induced regioselective and diastereoselective [3 + 2] cycloadditions

of nitrile oxides with some dipolarophiles to afford fused or spirocyclic isoxazolines.[31–33]

In the present study *N*,*α*-diphenyl nitrones were reacted with *N*-aryl maleimides in benzene to afford isoxazolidines. Recrystallization from suitable solvents furnished pure *cis*- or *trans*-stereoisomer in fairly good yields. However, *cis*/*trans* diastereomer mixture with ratio (55/45) was obtained in the case of both long-chained reagents. Intermolecular H-bonding plays a crucial role in the case of *cis*-diastereoselectivity. Density functional theory (DFT) calculations reveal that [3 + 2] cycloadditions proceeds via one step, but strongly asynchronous mechanism.

2 | EXPERIMENTAL

2.1 | Materials

All reagents and solvents were purchased from either Merck or Sigma-Aldrich (St. Louis, MO) and used without further purification. Thin-layer chromatography was performed using silica gel (60 F_{254}, Merck, Darmstadt, Germany) plates. Melting points were recorded by BÜCHI melting point B-540 apparatus (BUCHI Labortechnik AG in Flawil, Switzerland). The NMR spectra were measured using A600a Agilent DD2 600 MHz NMR spectrometer (Santa Clara, California, USA) dimethyl sulfoxide (DMSO)-d_6 using tetramethylsilane (TMS) as an internal standard. Chemical shifts (δ) are reported in ppm and *J* values in Hertz. The starting compounds **1**,[34] **2a**,[35] **3b**,[36] **4**,[37] and **5a**-**c**[38] were prepared according to reported procedures.

2.1.1 | *(Z)-1-(4-((11-Hydroxyundecyl)oxy)phenyl)-N-phenylmethanimine oxide* (**3a**)

In a 100-mL flask aldehyde **2a** (4.31 g, 1.47 mmol/L) and β-phenylhydroxylamine (1.61 g, 1.48 mmol/L) were dissolved in EtOH (15 mL). The flask was sealed and allowed to stand for 48 hours in the dark. Thereafter, the obtained bright yellow crystals were filtered under vacuum to afford **3a**. Yield 3.91 g, 69%. Mp: 111-112°C; IR (ATR): ν_{max} 3369, 3060, 2917, 2850, 1603, 1554, 1507, 1472, 1459, 1420, 1397, 1307, 1256, 1184, 1112, 1064, 1022, 942, 914, 893, 843, 807, 757, 719, 684, 634 cm^{-1}; ^1H NMR (600 MHz, DMSO-d_6) δ 8.40 (*d*, *J* = 9.0 Hz, 2H, Ar), 8.20 (*s*, 1H, =CH–), 7.81 (*d*, *J* = 7.8 Hz, 2H, Ar), 7.45-7.39 (*m*, 3H, Ar), 6.93 (*d*, *J* = 9.0 Hz, 2H, Ar), 4.16 (*t*, *J* = 4.8 Hz, 1H, −OH), 3.98 (*t*, *J* = 6.6 Hz, 2H, $PhOCH_2CH_2$–), 3.38 (*q*, *J* = 6.6 Hz, 2H, $-CH_2CH_2OH$), 1.72 (*quin*, *J* = 6.6 Hz, 2H, $PhOCH_2CH_2CH_2$–), 1.40 (*quin*, *J* = 6.6 Hz, 2 × 2H, $-CH_2CH_2CH_2OH$ and $PhOCH_2CH_2CH_2$–), 1.31-1.23 (*m*, 12H, *quin*, 6×–CH_2–); ^{13}C NMR (150 MHz, DMSO-d_6) δ 160.85, 148.78, 133.65, 131.31, 129.61, 129.13, 124.02, 121.57, 114.44, 68.05, 61.49, 32.97, 29.57, 29.47, 29.46, 29.45, 29.28, 29.09, 25.95, 25.94; Anal calc for $C_{24}H_{33}NO_3$ (383.53): C 75.16, H 8.67, N 3.65. Found: C 75.18, H 8.65, N 3.68.

2.1.2 | *4-(2,5-Dioxo-2,5-dihydro-1H-pyrrol-1-yl)-N-dodecylbenzamide* (**5d**)

In a 50-mL 2-necked flask fitted with a reflux condenser (protected by a $CaCl_2$ guard tube), dodecylamine (0.98 g, 5.29 mmol/L) and NEt_3 (0.74 mL, 5.31 mmol/L) were dissolved in (15 mL) $CHCl_3$ and cooled to 0°C. Acyl chloride **4** (1.25 g, 5.31 mmol/L) in (15 mL) $CHCl_3$ was added dropwise over 30 minutes. The resulting mixture was stirred at room temperature for 4 hours. Thereafter, the reaction mixture was washed successively with 2 × 15 mL of 0.1M HCl and H_2O (25 mL). The organic phase was dried over anhydrous Na_2SO_4, and the solvent was removed on a rotary evaporator. The residue was crystallized from hexane/EtOAc to afford white solid product. Yield 1.01 g, 49%. Mp: 169-171°C; IR (ATR): ν_{max} 3328, 3103, 3074, 2921, 2848, 1776, 1702, 1629, 1609, 1580, 1535, 1505, 1464, 1396, 1324, 1303, 1256, 1210, 1156, 1108, 1058, 1037, 1020, 950, 870, 851, 834, 771, 711, 687, 631, 619 cm^{-1}; ^1H NMR (600 MHz, DMSO-d_6) δ 8.50 (*t*, *J* = 5.4 Hz, 1H, −NH), 7.90 (*d*, *J* = 8.4 Hz, 2H, Ar), 7.41 (*d*, *J* = 8.4 Hz, 2H, Ar), 7.16 (*s*, 2H, −CH=CH–), 3.23 (*q*, *J* = 6.6 Hz, 2H, $-CH_2NH$–), 1.49 (*quin*, *J* = 6.6 Hz, 2H, $-CH_2CH_2CH_2NH$–), 1.26-1.15 (*m*, 18H, 9×–CH_2–), 0.82 (*t*, *J* = 6.6 Hz, 3H, $-CH_3$); ^{13}C NMR (150 MHz, DMSO-d_6) δ 170.10, 165.92, 135.21, 134.25, 134.13, 128.14, 126.55, 45.05, 31.72, 29.45, 29.43, 29.42, 29.19, 29.13, 26.89, 22.52, 14.37, 8.96; Anal calc for $C_{23}H_{32}N_2O_3$ (384.52): C 71.84, H 8.39, N 7.29. Found: C 71.83, H 8.41, N 7.27.

2.1.3 | *Typical experimental procedure for the synthesis of isoxazolidines* (**6a**-**d**, **7**)

In a 100-mL flask nitrone **3a** (0.49 g, 1.28 mmol/L) and maleimide **5b** (0.24 g, 1.28 mmol/L) were dissolved in (15 mL) of benzene. The flask was heated at 70°C for 3.5 hours, at which point thin layer chromatography (TLC) (7:3, Hexane:EtOAc) indicated complete consumption of the nitrone. Thereafter, the solvent was removed with rotary evaporator and the residue was crystallized from MeOH/EtOAc.

2.1.4 | *cis-3-(4-((11-Hydroxyundecyl)oxy)phenyl)-2,5-diphenyltetrahydro-4H-pyrrolo[3,4-d]isoxazole-4,6(5H)-dione* (**6a**)

Yield 75%, white crystalline solid, mp: 173.5-174.5°C; IR (ATR): ν_{max} 3549, 3066, 2919, 2850, 1799, 1713, 1611, 1598, 1511, 1489, 1455, 1392, 1312, 1292, 1246, 1181, 1099, 1051, 1028, 960, 930, 889, 851, 823, 758, 739, 722, 692, 630, 588 cm^{-1}; ^1H NMR (600 MHz, DMSO-d_6) δ 7.45 (t, *J* = 7.8 Hz, 2H, Ar), 7.39 (*t*, *J* = 7.8 Hz, 1H, Ar), 7.31 (*d*, *J* = 9.0 Hz, 2H, Ar), 7.24 (*t*, *J* = 7.8 Hz, 2H, Ar), 7.09-7.04 (*m*, 5H, Ar), 6.88 (*d*, *J* = 8.4 Hz, 2H, Ar), 5.39 (*d*, *J* = 7.8 Hz, 1H, H^3), 4.94 (*d*, *J* = 7.8 Hz, 1H, H^{6a}),

4.31 (*t*, *J* = 5.4 Hz, 1H, −OH), 4.12 (*t*, *J* = 7.8 Hz, 1H, H^{3a}), 3.90 (*t*, *J* = 6.6 Hz, 2H, $PhOCH_2CH_2$–), 3.36 (*q*, *J* = 6.6 Hz, 2H, $-CH_2CH_2OH$), 1.66 (*quin*, *J* = 6.6 Hz, 2H, $PhOCH_2CH_2CH_2$–), 1.40-1.35 (*m*, 4H, 2×–CH_2–), 1.29-1.24 (*m*, 12H, 6×–CH_2–); ^{13}C NMR (150 MHz, DMSO-d_6) δ 174.71, 172.45, 158.92, 148.01, 132.23, 129.40, 129.27, 129.13, 128.92, 127.32, 126.99, 125.00, 119.61, 114,85, 77.72, 70.61, 67.81, 61.19, 54.89, 33.01, 29.55, 29.47, 29.44, 29.42, 29.26, 29.16, 26.00, 25.97; Anal calc for $C_{34}H_{40}N_2O_5$ (556.70): C 73.36, H 7.24, N 5.03. Found: C 73.35, H 7.26, N 5.01.

2.1.5 | *cis-3-(4-((11-Hydroxyundecyl)oxy)phenyl)-2-phenyl-5-(p-tolyl)tetrahydro-4H-pyrrolo[3,4-d]isoxazole-4,6(5H)-dione* (6b)

Yield 89%, white solid, mp: 164.5-165°C; IR (ATR): ν_{max} 3547, 3065, 3034, 2921, 2851, 1797, 1717, 1610, 1599, 1583, 1512, 1490, 1467, 1396, 1313, 1290, 1247, 1184, 1111, 1095, 1047, 1022, 996, 967, 890, 853, 814, 756, 738, 690, 652, 611, 572 cm^{-1}; ^{1}H NMR (600 MHz, DMSO-d_6) δ 7.30 (*d*, *J* = 9.0 Hz, 2H, Ar), 7.24 (*t*, *J* = 7.8 Hz, 4H, Ar), 7.05 (*t*, *J* = 8.4 Hz, 3H, Ar), 6.95 (*d*, *J* = 7.8 Hz, 2H, Ar), 6.88 (*d*, *J* = 8.4 Hz, 2H, Ar), 5.38 (*d*, *J* = 7.8 Hz, 1H, H^3), 4.94 (*d*, *J* = 8.4 Hz, 1H, H^{6a}), 4.31 (*t*, *J* = 5.4 Hz, 1H, −OH), 4.10 (*t*, *J* = 8.4 Hz, 1H, H^{3a}), 3.90 (*t*, *J* = 6.6 Hz, 2H, $PhOCH_2CH_2$–), 3.36 (*q*, *J* = 6.6 Hz, 2H, $-CH_2CH_2OH$), 2.30 (*s*, 3H, $-CH_3$), 1.67 (*quin*, *J* = 6.6 Hz, 2H, $PhOCH_2CH_2CH_2$–), 1.40–1.35 (*m*, 4H, 2×–CH_2–), 1.29–1.24 (*m*, 12H, 6×–CH_2–); ^{13}C NMR (150 MHz, DMSO-d_6) δ 174.71, 172.47, 158.91, 148.08, 138.45, 132.23, 129.83, 129.63, 129.27, 129.13, 127.37, 126.73, 124.92, 119.48, 114,82, 77.71, 70.59, 67.81, 61.19, 54.85, 33.02, 29.57, 29.49, 29.45, 29.43, 29.28, 29.16, 26.01, 25.97, 21.14; Anal calc for $C_{35}H_{42}N_2O_5$ (570.73): C 73.66, H 7.42, N 4.91. Found: C 73.65, H 7.40, N 4.93.

2.1.6 | *cis-3-(4-((11-Hydroxyundecyl)oxy)phenyl)-4,6-dioxo-2-phenylhexahydro-5H-pyrrolo[3,4-d]isoxazol-5-yl)benzoic acid* (6c)

Yield 78%, white solid, mp: 172°C (dec.); IR (ATR): ν_{max} 3445, 3074, 2923, 2851, 1785, 1717, 1686, 1609, 1597, 1514, 1491, 1469, 1430, 1377, 1321, 1299, 1247, 1178, 1129, 1108, 1049, 1017, 959, 923, 892, 857, 819, 778, 757, 724, 691, 663, 611, 581 cm^{-1}; ^{1}H NMR (600 MHz, DMSO-d_6) δ 8.03 (*d*, *J* = 8.4 Hz, 2H, Ar), 7.30 (*d*, *J* = 9.0 Hz, 2H, Ar), 7.25-7.22 (*m*, 4H, Ar), 7.06-7.04 (*m*, 3H, Ar), 6.88 (*d*, *J* = 9.0 Hz, 2H, Ar), 5.40 (*d*, *J* = 7.8 Hz, 1H, H^3), 4.92 (*d*, *J* = 8.4 Hz, 1H, H^{6a}), 4.14 (*t*, *J* = 8.4 Hz, 1H, H^{3a}), 3.90-3.87 (*m*, 2H, $PhOCH_2CH_2$–), 3.36 (*q*, *J* = 6.6 Hz, 2H, $-CH_2CH_2OH$), 1.65 (*quin*, *J* = 7.2 Hz, 2H, $PhOCH_2CH_2CH_2$–), 1.38–1.36 (*m*, 4H, 2×–CH_2–), 1.28–1.22 (*m*, 12H, 6×–CH_2–); ^{13}C NMR (150 MHz, DMSO-d_6) δ 174.59, 172.24, 167.02, 158.96, 147.84, 135.88, 131.11, 130.44, 129.22, 129.12, 127.13, 126.91, 125.15, 119.82, 114.91, 77.72, 70.68, 67.81, 61.21, 54.96, 32.95, 29.53, 29.45, 29.41, 29.40, 29.25, 29.13, 25.99, 25.94; Anal calc for $C_{35}H_{40}N_2O_7$ (600.71): C 69.98, H 6.71, N 4.66. Found: C 69.99, H 6.69, N 4.68.

2.1.7 | *N-Dodecyl-4-(3-(4-((11-hydroxyundecyl)oxy)phenyl)-4,6-dioxo-2-phenylhexahydro-5H-pyrrolo[3,4-d]isoxazol-5-yl) benzamide* (6d)

Yield 80%, beige solid, mp: 129-130°C; IR (ATR): ν_{max} 3348, 3275, 3069, 2921, 2852, 1785, 1716, 1634, 1611, 1583, 1549, 1508, 1490, 1467, 1390, 1305, 1293, 1246, 1179, 1111, 1085, 1033, 1019, 959, 923, 895, 827, 804, 759, 721, 692, 623 ,591 cm^{-1}; ^{1}H NMR (600 MHz, DMSO-d_6) δ 8.49–8.45 (*m*, 1H, −NH), 7.89 (*d*, *J* = 8.4 Hz, 1H, Ar), 7.81 (*d*, *J* = 8.4 Hz, 1H, Ar), 7.43 (*d*, *J* = 8.4 Hz, 1H, Ar), 7.31 (*d*, *J* = 8.4 Hz, 1H, Ar), 7.25-7.20 (*m*, 2H, Ar), 7.17-7.15 (*m*, 2H, Ar), 7.05 (*t*, *J* = 8.4 Hz, 2H, Ar), 6.91 (*t*, *J* = 8.4 Hz, 1H, Ar), 6.88 (*d*, *J* = 8.4 Hz, 1H, Ar), 6.75 (*d*, *J* = 8.4 Hz, 1H, Ar), 5.75 (*s*, 1H, *trans*-H^3), 5.41 (*t*, *J* = 7.2 Hz, 1H, *cis*-H^3), 4.94 (*d*, *J* = 8.4 Hz, 1H, H^{6a}), 4.31–4.29 (*m*, 1H, −OH), 4.14 (*t*, *J* = 8.4 Hz, 1H, H^{3a}), 3.94-3.89 (*m*, 2H, $PhOCH_2CH_2$–), 3.38-3.34 (*m*, 2H, $-CH_2CH_2OH$), 3.25-3.20 (*m*, 2H, $-CH_2NH$–), 1.70-1.64 (*m*, 2H, $PhOCH_2CH_2CH_2$–), 1.52-1.45 (*m*, 2H, $-CH_2CH_2CH_2NH$–), 1.40-1.35 (*m*, 4H, 2×–CH_2–), 1.30-1.23 (*m*, 24H, 12×–CH_2–); 0.84-0.82 (*m*, 3H, $-CH_3$); ^{13}C NMR (150 MHz, DMSO-d_6) δ 174.82, 174.52, 173.60, 172.25, 165.74, 165.64, 158.95, 158.69, 149.23, 147.99, 135.29, 135.15, 134.28, 134.02, 131.32, 129.40, 129.24, 129.12, 128.85, 128.25, 128.08, 127.29, 126.60, 126.53, 124.97, 122.61, 119.56, 114.87, 114.86, 114.77, 78.12, 77.77, 70.60, 68.67, 67.88, 67.82, 61.18, 57.04, 54.96, 46.05, 33.02, 31.76, 29.57, 29.56, 29.52, 29.48, 29.46, 29.44, 29.30, 29.26, 29.18, 29.14, 26.93, 26.01, 25.98, 22.56, 14.38; Anal calc for $C_{47}H_{65}N_3O_6$ (768.05): C 73.50, H 8.53, N 5.47. Found: C 73.49, H 8.55, N 5.49.

2.1.8 | *trans-4-(4,6-Dioxo-2,3-diphenylhexahydro-5H-pyrrolo[3,4-d]isoxazol-5-yl)-N-dodecylbenzamide* (7)

Yield 93%, white solid, mp: 156-157°C; IR (ATR): ν_{max} 3259, 3064, 3035, 2924, 2853, 1782, 1714, 1638, 1616, 1544, 1506, 1489, 1467, 1451, 1386, 1306, 1259, 1190, 1112, 1078, 1059, 1017, 950, 903, 857, 835, 763, 723, 695, 627 cm^{-1}; ^{1}H NMR (600 MHz, DMSO-d_6) δ 8.45 (*t*, *J* = 5.4 Hz, 1H, −NH), 7.80 (*d*, *J* = 8.4 Hz, 2H, Ar), 7.55 (*d*, *J* = 7.2 Hz, 2H, Ar), 7.40 (*t*, *J* = 7.2 Hz, 2H, Ar), 7.32 (*t*, *J* = 7.2 Hz, 1H, Ar), 7.23 (*t*, *J* = 7.2 Hz, 2H, Ar), 7.19 (*d*, *J* = 7.8 Hz, 2H, Ar), 6.93 (*t*, *J* = 7.2 Hz, 1H, Ar), 6.71 (*d*, *J* = 8.4 Hz, 2H, Ar), 5.85 (*s*, 1H, H^3), 5.41 (*d*, *J* = 7.8 Hz, 1H, H^{6a}), 4.13 (*d*, *J* = 7.8 Hz, 1H, H^{3a}), 3.23–3.20 (*m*, 2H, $-CH_2NH$–), 1.48 (*quin*, *J* = 6.6 Hz, 2H, $-CH_2CH_2CH_2NH$–), 1.26–1.23 (*m*, 18H, 9×–CH_2–), 0.84 (*t*, *J* = 6.6 Hz, 3H, $-CH_3$); ^{13}C NMR (150 MHz, DMSO-d_6) δ 174.76, 173.52, 165.64, 149.38, 139.55, 135.33, 133.98, 129.49, 129.02, 128.26, 128.07, 127.49, 126.53, 122.73, 114.72, 78.25, 69.05, 57.03, 31.75, 29.50, 29.47, 29.23, 29.16, 26.91, 22.55, 14.40; Anal calc for

$C_{36}H_{43}N_3O_4$ (581.76): C 74.33, H 7.45, N 7.22. Found: C 74.35, H 7.43, N 7.21.

3 | RESULTS AND DISCUSSION

The known starting materials, **1**,[34] **2a**,[35] **3b**,[36] **4**,[37] and **5a-c**[38] were prepared according to the literature procedures. Nitrone **3a** and long-chained *N*-substituted maleimide **5d** used in this study were prepared according to the general routes shown in Schemes 1 and 2, respectively. The newly synthesized compounds **3a** and **5d** were characterized by Infrared (IR), NMR spectroscopic techniques, and elemental analysis. For the general cycloaddition reaction, the corresponding nitrones and maleimides was heated in benzene for 3.5 hours at 70°C. Thereafter, the reaction mixture was concentrated under vacuum and the obtained solid was recrystallized from suitable solvent to give a single diastereomer in fairly good yield (Table 1).

The cycloaddition reaction of *N*-phenyl-*α*-(p-(11-hydroxy)undecyloxyphenyl)nitrone with *N*-arylmaleimides gave only (*syn*) *cis*-diastereomers as a product. On the other hand, the reaction of *N*-phenyl-*α*-phenylnitrone with *N*-(4-dodecylcarbamoylphenyl)maleimide gave only (*anti*) *trans*-diastereomer as a product (Scheme 3). However, *cis*/*trans*-diastereomers mixture was obtained when the cycloaddition reaction was performed between the *N*-phenyl-*α*-(p-(11-hydroxy)undecyloxyphenyl)nitrone and *N*-(4-dodecylcarbamoylphenyl)maleimide.

In these reactions, the *cis*- or *trans*-diastereoselectivity arises from the noncovalent interactions at the transition states. The *cis* selectivity is substantially controlled by the 11-hydroxyundecyloxy group on the phenyl ring of nitrone **3a**. The molecule can adopt a number of different conformational shapes. Thus, it can be proposed that the flexible hydrocarbon chain of the nitrone is capable of adopting suitable interaction conformation throughout *exo-Z* transition state (Figure 1). In the case of the *exo-Z* transition state, the DFT results confirm that the cycloaddition proceeded through this state, wherein hydroxyl group at the end of the hydrocarbon chain forms a hydrogen bond with the carbonyl functional group of the maleimide making this state favorable.[39–42] According to Praly et al,[39] chiral nitrones with racemic 3-substituted butenes give H-bonding–induced diastereoselective intermolecular [3 + 2] cycloadditions via *exo*-transition state predominantly. On the other hand, Sadownik and Philip[40] demonstrated that some nitrones and maleimides can afford *cis*-isoxazolidines via transition states including intermolecular H-bonding. Therefore, these studies in the literature, supporting the high diastereoselectivity in [3 + 2] cycloaddition reactions performed in this study.

Endo-E transition state is another possible transition state on the reaction route to the *cis*-diastereomer (Figure 1). The *secondary orbital interactions*, noncovalent attractive interactions between the *N*-bonded aromatic rings belonging to the *E*-nitrone and the maleimide can cause the reaction to proceed via this transition state.[4,13,43–45] There are large numbers of studies that support cycloaddition reactions via *E*-nitrones.[46–51] However, their sandwich interaction is largely unfavorable and computational calculations reveal that *exo-Z* is the more favorable transition state. On the other hand, one may expect high repulsion between the voluminous 11-hydroxyundecyloxy substituent and aryl group of maleimide in the *exo-Z* and *endo-E* transition states. If the steric factors were decisive in the reaction of the nitrone **3a** with maleimides **5a-c**, the *exo-E* or *endo-Z* must be the preferred transition states furnishing the *trans*-isoxazolidine dia-

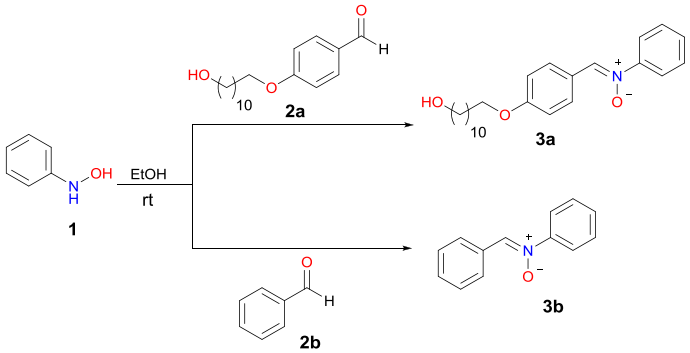

SCHEME 1 Synthesis of nitrones **3a** and **3b**

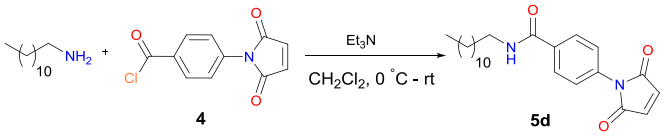

SCHEME 2 Synthesis of maleimide **5d**

TABLE 1 [3 + 2] Cycloaddition of azomethine-*N*-oxides with *N*-aryl substituted maleimides

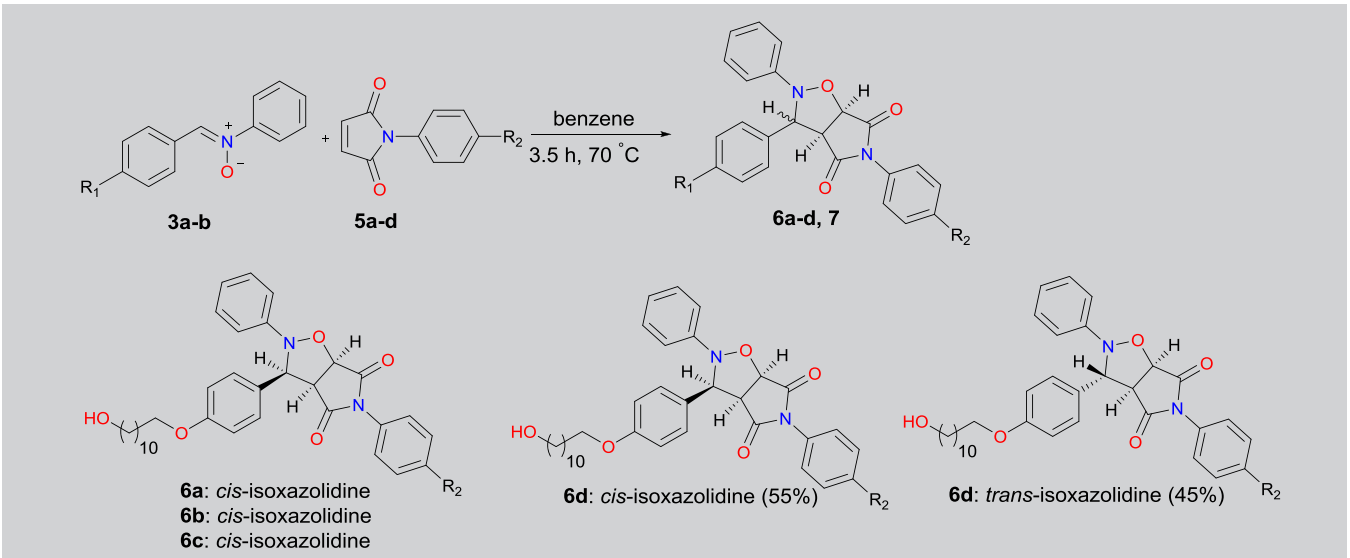

Entry	Nitrone	Maleimide	R_1	R_2	Diastereomer	Yield %[a]
1	**3a**	**5a**	$O(CH_2)_{11}OH$	H	*cis*-**6a**	75
2	**3a**	**5b**	$O(CH_2)_{11}OH$	CH_3	*cis*-**6b**	89
3	**3a**	**5c**	$O(CH_2)_{11}OH$	COOH	*cis*-**6c**	78
4	**3a**	**5d**	$O(CH_2)_{11}OH$	$CONH(CH_2)_{11}CH_3$	*cis/trans*-**6d** (55/45)	80
5	**3b**	**5d**	H	$CONH(CH_2)_{11}CH_3$	*trans*-**7**	93

[a]Yields after recrystallization.

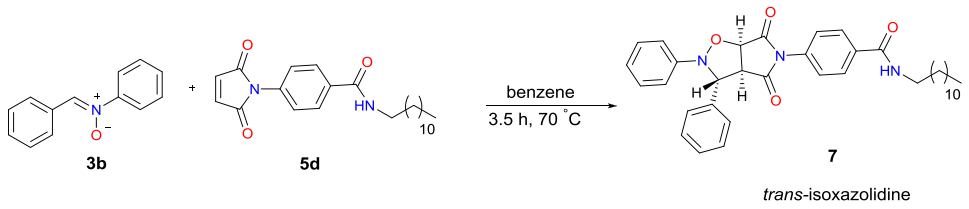

SCHEME 3 Synthesis of isoxazolidine **7**

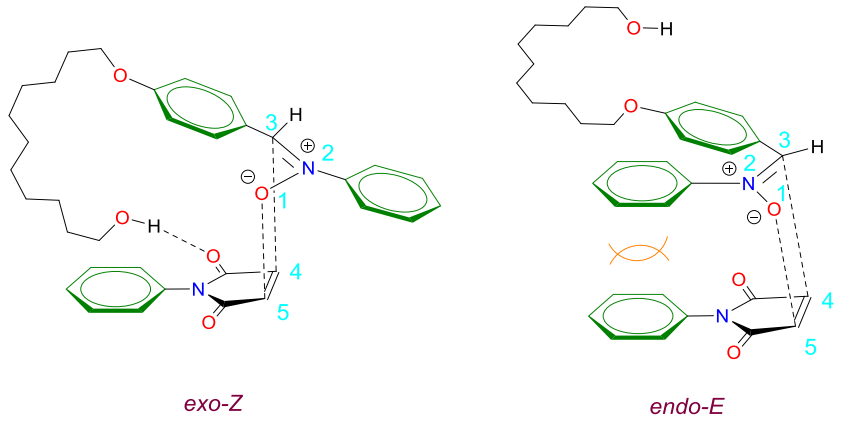

FIGURE 1 Trajectories of transitions states leading to *cis*-isoxazolidines

stereomer. But the NMR result reveals the *cis*-isoxazolidine as a single product. As reported previously, only *Z* configuration has been shown to actually exist for aldonitrones by UV, IR, and NMR spectroscopy.[52] Accordingly, only one signal was observed at δ 8.20 ppm as a methine proton in the NMR spectrum of the nitrone **3a**.

In the case of *trans* selectivity the cycloaddition is controlled possibly by 2 factors, one of which is the absence of the steric repulsion effect between the long-chained dodecylcarbamoyl moiety of the maleimide and phenyl rings of the *E*-nitrone. This factor can cause the cycloaddition reaction to proceed via the *exo-E* transition state (Figure 2).

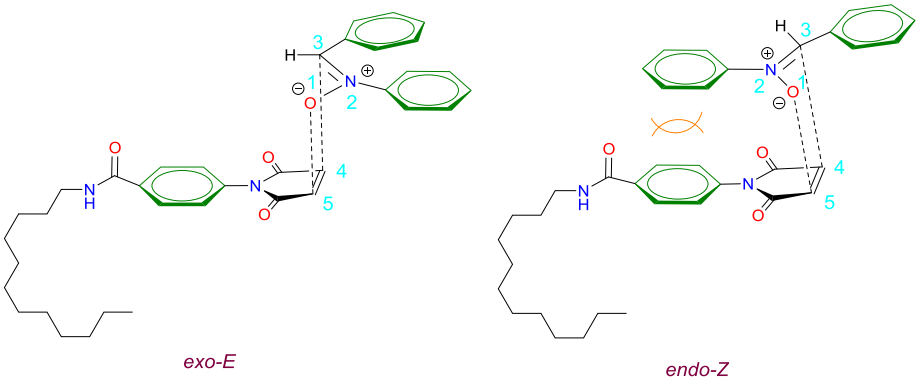

FIGURE 2 Trajectories of transitions states leading to *trans*-isoxazolidines

Another factor that may affect the transition state is the *(secondary orbital interactions)* noncovalent attractive interactions between the *N*-bonded aromatic ring of *Z*-nitrone and maleimide aromatic ring that can lead the reaction to proceed via the *endo-Z* transition state (Figure 2). However, it is not the possible transition state because of *sandwich repulsion*. A computational analysis reveals that the *trans*-diastereoisomer was obtained via the more preferred *exo-E* transition state.

The stereochemistry of the cycloadduct was determined from the peak splitting patterns and coupling constants related to isoxazolidine ring protons numbered as H^3, H^{3a}, and H^{6a} (Figure 3).

The spin multiplicities of these protons are decisive for the *cis*- and *trans*-diastereomers. The evaluation of ^1H NMR spectra of the obtained *cis*-stereoisomers (H^3, H^{3a} *syn*-relationship) showed that H^3 protons have chemical shift between 5.38 and 5.40 ppm giving a doublet peak. The cycloadducts **6a-c**, showed $J_{3\text{-}3a}$ = 7.8 Hz, which is in the range expected of a H^3, H^{3a} *syn*-relationship. The H^{6a} protons have chemical shift between 4.92 and 4.94 ppm giving a doublet peak and H^{3a} protons have chemical shift between 4.14 and 4.10 ppm giving a pseudo triplet instead of doublet of doublet peak (Figure 4A).

The evaluation of ^1H NMR spectra of the obtained *trans*-stereoisomers (H^3, H^{3a} *trans*-relationship) showed that H^3 protons have chemical shift at 5.75 or 5.85 ppm and appears as a singlet peak (Figure 4B). This peak proves that

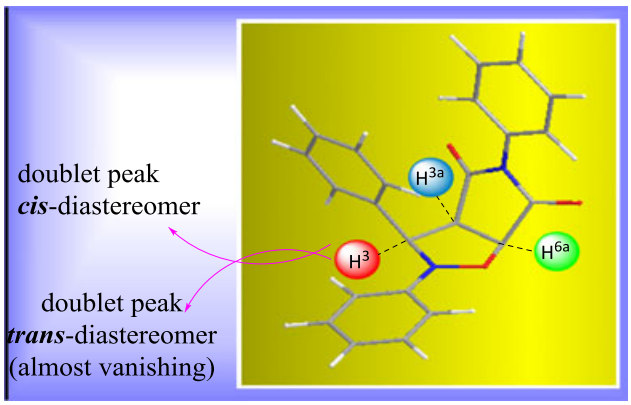

FIGURE 3 Diagnostic hydrogen atoms of diastereomers

H^3 proton and H^{3a}, H^{6a} protons are in the *anti*position and the spin-spin coupling between H^3 proton and H^{3a} could not be seen. Additionally, H^{6a} protons have chemical shift at 5.41 ppm giving a doublet or triplet peak and H^{3a} protons have chemical shift between 4.13 and 4.14 ppm giving a doublet peak (triplet for the compound **6d**). The spectra also clearly showed the spin-spin coupling of H^{3a} and H^{6a} protons. The *cis*/*trans* ratio for the isoxazolidine **6d**, was determined by integration of signals assigned to each diastereomer in the ^1H NMR spectra. A 55/45 *cis*/*trans* ratio was obtained by integrating the *cis* and *trans* H^3 protons at 5.41 and 5.75 ppm, respectively.

3.1 | Computational method

In the present work, the Becke-Lee-Yang-Parr functional (B3LYP) method[53] using 6-31G and 6-311G(d,p) basis sets were adopted and all calculations were performed using the GAUSSIAN 09 program package.[54] Harmonic frequencies of the structures were calculated at the same method and basis sets to find local minima (all positive force constants) or transition states (one imaginary force constant only). The intrinsic reaction coordinate calculation has been used to verify the true transition structure. For the calculations of solvent effect on the reaction paths, the polarizable continuum model,[55] in which the cavity is created via a series of overlapping spheres, was used. As the DFT functional poorly describe dispersion effects, dispersion correction for reaction heat and free energy barrier were also estimated using the wB97X-D/6-311G(d,p) method developed by Grimme and coworkers.[56]

The global electrophilicity index, ω is given by the following expression[57] ($\omega = \mu^2/2\eta$), in terms of the electronic chemical potential μ and the chemical hardness η. Both quantities may be approached in terms of the one-electron energies of the frontier molecular orbitals (FMOs) highest occupied molecular orbital (HOMO) and lowest unoccupied molecular orbital (LUMO), ε_H and ε_L, as $\mu \cong -(\varepsilon_H + \varepsilon_L)/2$ and $\eta \cong (\varepsilon_L - \varepsilon_H)/2$, respectively. Global softness, S, is related to global hardness and is given by the inverse of 2η.[58]

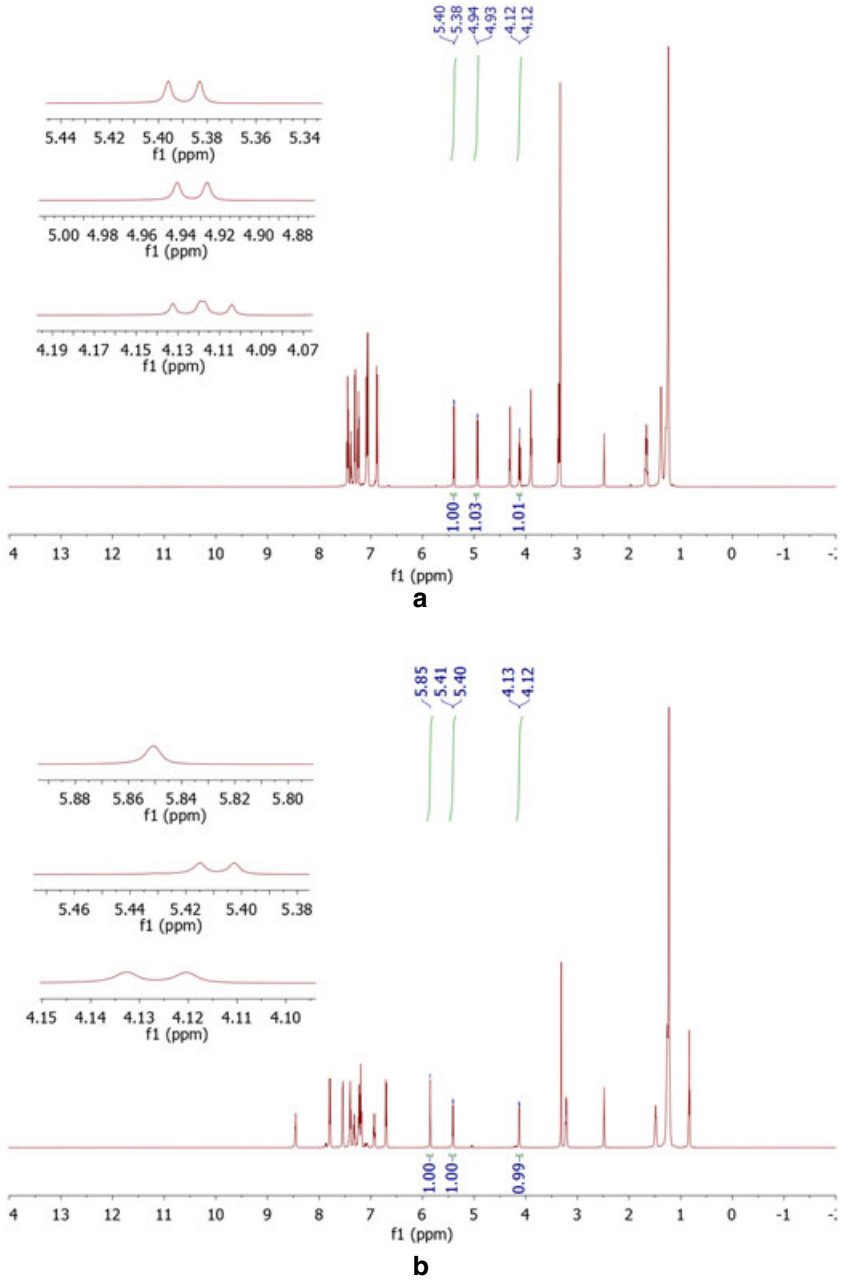

FIGURE 4 (A) 1H nuclear magnetic resonance (NMR) spectra of compound **6a**. (B) 1H NMR spectra of compound **7**

All calculations were performed at 298 K and pressure of 1 atm. Absolute entropies of critical structures (*S*) were estimated from complete vibrational analysis. Enthalpies (*H*) were corrected to Gibbs free energies (*G*) using calculated entropies.

3.2 | Frontier molecular orbitals

All of the molecules were optimized by DFT/B3LYP method and 6-31G basis set. The calculated optimized free energies of nitrones **3a** and **3b** and maleimides **5a-d** has been provided in Table 2.

The HOMOs and LUMOs are known as FMOs which played an important role for evaluating molecular chemical stability, chemical reactivity, and hardness-softness of the molecule.[57] The HOMO and LUMO energy and energy gap (ΔE) absolute electronegativity (χ), chemical hardness (η), softness (S), and electrophilicity index (ω) of the nitrones and the maleimides are listed in Table 2.[59,60] The HOMO and LUMO energies of nitrone, which is **3a**, are lowered by 0.381 and 0.190 eV, respectively, compared with **3b**. The HOMO acts as an electron donor, while the LUMO is an electron acceptor. The energy gap (ΔE) represents the chemical reactivity of compounds. For a system lower value of ΔE makes it more reactive or less stable. The HOMO/LUMO energy gaps for the cycloaddition reactions of nitrones **3a** and **3b** to maleimides **5a**-**d** have been listed in Table 3.

The energy differences indicate that $HOMO_{nitrone}$-$LUMO_{maleimide}$ interaction results in a lower gap than $HOMO_{maleimide}$-$LUMO_{nitrone}$ interaction; hence, the former

TABLE 2 Highest occupied molecular orbital (HOMO) and lowest unoccupied molecular orbital (LUMO) energies, the energy gap (ΔE), absolute electronegativity (χ), chemical hardness (η), softness (S), and electrophilicity index (ω) of nitrones **3a** and **3b** and maleimides **5a-d** using B3LYP/6-31G level

Compound Global Reactivity Descriptors	3a	3b	5a	5b	5c	5d
E (HOMO, a.u.)	−0.189	−0.195	−0.261	−0.250	−0.254	−0.253
E (LUMO, a.u.)	−0.059	−0.066	−0.107	−0.105	−0.122	−0.118
ΔE, eV	3.54	3.51	4.19	3.94	3.59	3.67
χ	−3.373	−3.550	−5.005	−4.828	−5.114	−5.046
η	1.768	1.754	2.094	1.972	1.795	1.836
S	0.28	0.29	0.24	0.25	0.28	0.27
ω	3.22	3.59	5.99	5.92	7.30	6.93

TABLE 3 The density functional theory/B3LYP-6-31G calculated highest occupied molecular orbital (HOMO)/lowest unoccupied molecular orbital (LUMO) energy gaps for the cycloaddition reactions of the nitrones and the maleimides

Reaction	$LUMO_{maleimide}$-$HOMO_{nitrone}$, eV	$LUMO_{nitrone}$-$HOMO_{maleimide}$, eV
6a (**3a** + **5a**)	2.230	5.494
6b (**3a** + **5b**)	2.285	5.195
6c (**3a** + **5c**)	1.822	5.304
6d (**3a** + **5d**)	1.931	5.277
7 (**3b** + **5d**)	2.094	5.086

is the predominant interaction involved in each case. This reveals a normal electron demand character of the cycloaddition reactions. The $HOMO_{nitrone}$-$LUMO_{maleimide}$ energy gap is least along the serials for the cycloaddition reactions of **3a** to **5a-d** and the largest for the reaction involving **3b**.

The energy gap, ΔE is directly involved with hardness/softness of a chemical species. The higher value of ΔE represents more hardness or less softness of compounds, the system having the maximum hardness being the most stable.[61] The global reactivity descriptor chemical potential (I), which is represented by HOMO energy, occurs from charge distribution between 2 systems having different chemical potential. Here, all compounds act as electrophiles, and hence, their electronic potentials (I) are negative. Another global reactivity descriptor electrophilicity index (ω) describes the electron accepting ability of the systems quite similar to η and I. High values of electrophilicity index increases electron accepting abilities of the molecules.

As depicted in Table 2, the electronic chemical potentials of the nitrones, **3a** (−3.373 eV) and **3b** (−3.550 eV) are higher than that of the maleimides, **5a-d** (−4.828 to −5.114 eV). On the other hand, the global hardness of the maleimides, **5a-d** (1.795 to 2.094 eV), is higher than that of the nitrones, **3a** and **3b** (1.768 and 1.754 eV, respectively). This predicts that the net charge transfer will take place from the nitrones to the maleimides in each case along the cycloaddition reactions. This is in complete agreement with the HOMO/LUMO energy gap predictions. The global electrophilicity indices of the maleimides are higher than those of the nitrones. This is in agreement with FMO and electronic chemical potential calculations. The global electrophilicity differences ($\Delta\omega$) between **3a** and **5a-d** and **3b** and **5d** are calculated at 2.767, 2.701, 4.077, 3.706, and 3.334, respectively. These results indicate that the least polar character for the cycloaddition reactions is **3a** to **5b**, while the highest global electrophilicity difference ($\Delta\omega$) was observed in the reaction of **3a** with **5c**.

The electron density in both FMOs, HOMO and LUMO of **3a** and **3b**, was collected on nitrone group and phenyl ring, while in the maleimides HOMO orbital this density is delocalized on phenyl ring and LUMO orbital is delocalized on maleimide group as shown in Figures S9 and S10.

3.3 | Molecular electrostatic potential map

The chemical reactivity of the compounds are easily determined with the help of molecular electrostatic potential map (MEP), which differentiates the electrophilic and nucleophilic sites in a molecule quite easily.[62] For this purpose the MEPs have been calculated for the nitrones and the maleimides at the B3LYP/6-31G level. In MEP plots as represented in Figure S11, the negative regions represented by red color are preferable sites for electrophilic attack and the positive regions represented by blue color are favored nucleophilic attack. Here, the negative potentials are generated over the electronegative nitrone O and N atoms, whereas the H-atoms of maleimide group in maleimides have the positive potential region in the structures. These negative and positive sites help to predict the regions in a compound responsible for noncovalent interactions.[63]

3.4 | Diastereoselectivity of the performed cycloaddition reactions

DFT is the more popular method in recent years in computational chemistry. It provides an appropriate level of theory and costs for a number of problems supporting experimental research. However, there is a limitation to describe dispersion effect. Therefore, DFT/B3LYP hybrid functional is not satisfactory to obtain reliable energies. Development has been done to treat this nontrivial matter. Excellent reviews on dispersion interactions in DFT are given by Johnson et al[64] and Grimme,[65] including the widely accepted scheme by Grimme of dispersion-corrected DFT that are DFT-D[66,67] and DFT-D3.[56] Therefore, all the calculations were first done on the B3LYP/6-311G(d,p) level, and then, they were

TABLE 4 Kinetic and thermodynamic parameters for the cycloaddition reactions of nitrones (**3a** and **3b**) with maleimides (**5a-d**) according to DFT calculations (T = 298 K)

Transition	B3LYP/6-311G(d,p)			W697X-D/6-311G(d,p)		
	Δ*H*, degrees (°)	Δ*S*, J/mol K	Δ*G*, kJ/mol	Δ*H*, degrees (°)	Δ*S*, J/mol K	Δ*G*, kJ/mol
3a + **5a** → TS_{EXO-Z}	82.4	−88.7	108.8	65.6	−76.4	88.4
3a + **5a** → TS_{ENDO-E}	165.7	−102.1	196.1	144.1	−88.4	170.5
3a + **5a** → $6a_{cis}$	−64.6	−166.2	−15.0	−45.7	−136.0	−5.2
3a + **5a** → TS_{EXO-E}	107.6	−84.5	132.8	85.6	−81.5	109.9
3a + **5a** → TS_{ENDO-Z}	130.5	−97.4	159.5	116.3	−85.9	141.9
3a + **5a** → $6a_{trans}$	−82.7	−174.5	−30.7	−66.9	−158.2	−19.7
3a + **5b** → TS_{EXO-Z}	75.9	−81.4	100.2	57.8	−72.4	79.4
3a + **5b** → TS_{ENDO-E}	145.5	−97.8	174.7	113.3	−81.8	137.7
3a + **5b** → $6b_{cis}$	−87.9	−161.0	−39.9	−55.9	−125.7	−18.4
3a + **5b** → TS_{EXO-E}	92.9	−79.7	116.7	75.1	−71.9	96.5
3a + **5b** → TS_{ENDO-Z}	106.6	−99.4	136.2	81.4	−88.3	107.7
3a + **5b** → $6b_{trans}$	−99.2	−167.2	−49.3	−69.3	−146.5	−25.6
3a + **5c** → TS_{EXO-Z}	94.2	−71.9	115.6	81.1	−62.0	99.6
3a + **5c** → TS_{ENDO-E}	148.1	−95.7	176.6	130.4	−81.4	154.7
3a + **5c** → $6c_{cis}$	−67.2	−160.1	−19.4	−45.2	−124.8	−8.0
3a + **5c** → TS_{EXO-E}	105.0	−87.4	131.1	85.1	−73.1	106.9
3a + **5c** → TS_{ENDO-Z}	114.7	−92.5	142.3	99.5	−80.4	123.5
3a + **5c** → $6c_{trans}$	−79.6	−163.7	−30.8	−66.4	−144.7	−23.3
3a + **5d** → TS_{EXO-Z}	87.2	−78.4	110.6	69.8	−66.1	89.5
3a + **5d** → TS_{ENDO-E}	141.0	−87.9	167.2	118.9	−74.9	141.2
3a + **5d** → $6d_{cis}$	−67.7	−159.4	−20.2	−50.4	−141.0	−8.4
3a + **5d** → TS_{EXO-E}	102.7	−82.5	127.3	77.5	−70.4	98.5
3a + **5d** → TS_{ENDO-Z}	118.7	−91.4	146.0	93.7	−82.5	118.3
3a + **5d** → $6d_{trans}$	−76.7	−167.6	−26.6	−56.2	−151.5	−11.0
3b + **5d** → TS_{EXO-Z}	101.3	−72.4	122.9	88.2	−58.7	105.7
3b + **5d** → TS_{ENDO-E}	160.7	−89.5	187.4	147.0	−77.2	170.0
3b + **5d** → 7_{cis}	−50.2	−157.2	−3.3	−40.4	−141.5	1.8
3b + **5d** → TS_{EXO-E}	86.9	−86.2	112.6	69.7	−80.4	93.7
3b + **5d** → TS_{ENDO-Z}	125.5	−90.4	152.5	113.2	−79.5	136.9
3b + **5d** → 7_{trans}	−56.2	−157.4	−9.3	−49.9	−144.7	−6.8

additionally performed by wB97X-D method using the 6-311G(d,p) basis set. Enthalpies (a.u.) of the reactants, transition states, and the products for the cycloaddition reactions of nitrones (**3a** and **3b**) with maleimides (**5a-d**) calculated at 298 K are given in Table S1, while the relative enthalpies, entropies, and free energies of all the molecules are listed in Table 4. The third and sixth column in Table 4 show the relative free energies calculated with B3LYP and wB97X-D, respectively, for all reactions, while the other columns present the relative enthalpies and entropies. In general, the relative free energies of all molecules calculated from wB97X-D are lower than those from the B3LYP level. All of the energy discussions are based on the wB97X-D method and 6-311G (d,p) basis set because of the inclusion of the dispersion effect.

The analysis of the Gibbs free energies of the transition states for the performed cycloaddition reaction reveals that the *exo-Z* and *exo-E* are less energetic than *endo-E* and *endo-Z* (Table 4). The relative Gibbs free energy of the reaction **3b** + **5d** → TS_{EXO-E} was calculated at 93.7 kJ/mol, which is lower than that of the other 3 pathways: **3b** + **5d** → TS_{EXO-Z}, **3b** + **5d** → TS_{ENDO-E}, **3b** + **5d** → TS_{ENDO-Z} (calcd. 105.7, 170.0, and 136.9 kJ/mol, respectively). This result shows that the molecule **7**, synthesized from **3b** and **5d** is the *trans* isomer. On the other hand, other molecules, **6a-d,** are adopted *cis* isomers, because their Gibbs free energies of transition state, TS_{EXO-Z}, are

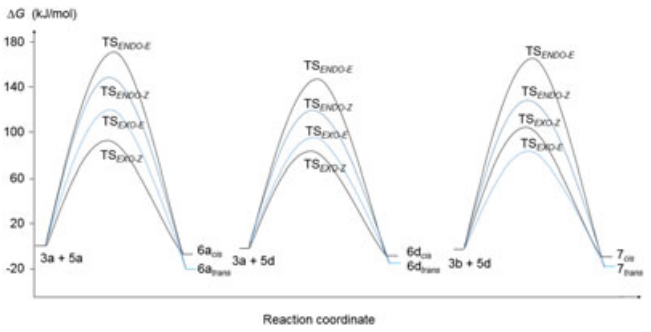

FIGURE 5 Reaction profiles for the cycloaddition reactions of nitrones (**3a** and **3b**) with maleimides (**5a** and **5d**)

lower than those of the other 3 pathways. The calculated free energies of $TS_{EXO\text{-}Z}$ of **6a-d** molecules are 88.4, 79.4, 99.6, and 89.5 kJ/mol, respectively. The energy profiles of the formation reaction of the compounds **6a**, **6d**, and **7** are shown in Figure 5.

Analysis of transition states geometries shows that the reaction course is determined by attack of the nucleophilic oxygen atom from the CNO moiety of nitrone onto the electrophilic center of dipolarophile. Similar tendency has been observed recently in other reactions involving diarylnitrones.[45,68]

The intermolecular H-bonding or repulsive interactions between phenyl rings makes the *exo* approaches more favorable (Figures 1 and 2). In *endo-E* and *endo-Z* transition states steric repulsion is possible between the phenyl ring of the maleimide and the *N*-phenyl ring of the nitrone. The optimized structures of the transition states *exo-Z* and *exo-E* respectively of the compounds **6a** and **7** are given in Figure 6. For **6a** the lengths of the C^5–O^1 and C^3–C^4 forming bonds are 2.060 and 1.984 A°, respectively, and the H-bond length is 2.388 A° at the transition state *exo-Z*. On the other hand, for **7** the lengths of the C^5-O^1 and C^3–C^4 forming bonds are 2.291 and 2.169 A°, respectively, at the transition state *exo-E*. The asynchronicity according to $\Delta r = [d(C^5\text{–}O^1) - d(C^3\text{–}C^4)]$[69] at the transition states during the formation of compound **6a** is 0.076 at *exo-Z* and 0.313 at *endo-E*, whereas the asynchronicity at the transition states during the formation of compound **7** is 0.122 at *exo-E* and 0.675 at *endo-Z*. Therefore, the more favorable transition states *exo-Z* (0.076) and *exo-E* (0.122) are more synchronous than transition states *endo-E* and *endo-Z*.

TABLE 5 Essential molecular properties of the molecules of the cycloaddition reactions of nitrones (**3a** and **3b**) with maleimides (**5a-d**) according to DFT calculations

Molecule	C^5–O^1		C^3–C^4		CT[b] (e)
	r, Å	I[a]	*r*, Å	*I*[a]	
3a + 5a	2.783		3.984		0.00
TSa	2.060	0.594	1.984	0.742	0.36
6a	1.465		1.577		
3a + 5b	2.614		3.956		0.00
TSb	2.087	0.576	2.001	0.732	0.41
6b	1.466		1.578		
3a + 5c	2.704		3.842		0.00
TSc	2.105	0.562	2.016	0.722	0.37
6c	1.464		1.578		
3a + 5d	2.711		3.927		0.00
TSd	2.247	0.466	2.101	0.667	0.38
6d	1.465		1.576		
3b + 5d	2.843		3.987		0.00
TS7	2.291	0.434	2.169	0.613	0.38
7	1.463		1.564		

[a]$I_{X-Y} = 1 - (r_{X-Y}^{TS} - r_{X-Y}^{3+5}/r_{X-Y}^{TS})$, where $r_{X\text{-}Y}^{TS}$ is the distance between the reaction centers *X* and *Y* in the transition structure and $r_{X\text{-}Y}^{3+5}$ is the same distance in the corresponding product.

[b]$CT = -\Sigma q_A$, where q_A is the net charge and the sum is taken over all the atoms of the dipolarophile.

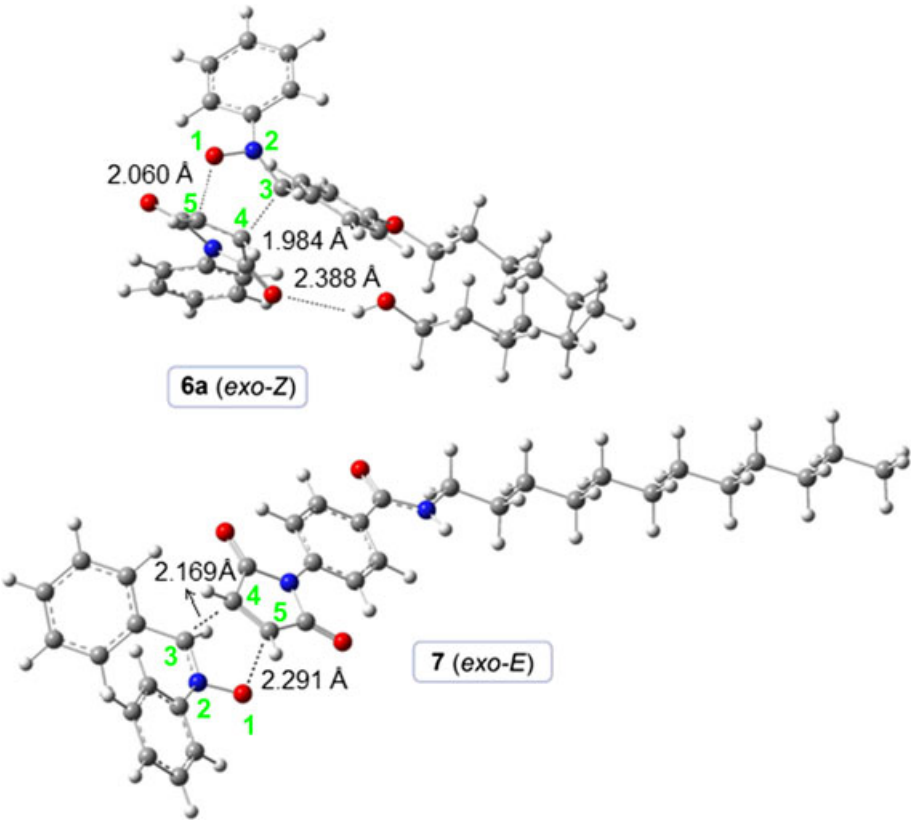

FIGURE 6 Optimized structures of transition states of **6a** (*exo-Z*) and **7** (*exo-E*)

According to another more realistic approach, global and local reactivity indices as distance between reaction centers of transition states and/or products also indicate a polar character of the cycloadditions (Table 5).[17] On the other hand, C^5–O^1 and C^3–C^4 bonds have different nature and different lengths. In consequence, an analysis of asynchronicity cannot directly compare these bonds in the transition states. The calculated lengths of the C^5–O^1 and C^3–C^4 forming bonds at the transition states are 2.060 and 1.984 Å at TSa, 2.087 and 2.001 Å at TSb, 2.105 and 2.016 Å at TSc, 2.247 and 2.101 Å at TSd, and 2.291 and 2.169 Å at TS7, respectively. These bond lengths indicate that these transition states correspond to an asynchronous single bond formation process in which the C^3–C^4 bond formation is more advanced than the C^5–O^1 one.

Thus, DFT calculations also reveal that cycloadditions proceed via one step, but strongly asynchronous mechanism. According to Domingo,[70] these reactions take place through a highly asynchronous transition state considered as "2-stage 1-step" *cycloaddition* instead of ideal pericyclic process.

4 | CONCLUSIONS

In the present work, both experimental and computational studies were performed in order to investigate the high diastereoselectivity controlled by intermolecular H-bonding in the cycloaddition of *N*-aryl substituted maleimides with selected two *N*,*α*-diphenyl nitrones. Depending on the reactants either *cis*- or *trans*-cycloadduct was obtained as a single diastereomer confirmed by NMR. The optimized transition state structures showed that *exo-Z* and *exo-E* are more synchronous and preferred than *endo-E* and *endo-Z* transition states. On the other hand, global and local reactivity indices as distance between reaction centers of transition states reveal that cycloaddition reactions takes place through 2-stage 1-step cycloaddition instead of ideal pericyclic process.

REFERENCES

[1] V. C. Allen, D. Philp, N. Spencer, *Org. Lett.* **2001**, *3*, 777.

[2] I. Blanáriková, B. Dugovic, L. Fišera, C. Hametner, N. Prónayová, *ARKIVOC* **2001**, *ii*, 109.

[3] H. Agirbas, S. Guner, F. Budak, S. Keceli, F. Kandemirli, N. Shvets, V. Kovalishynd, A. Dimoglo, *Bioorg. Med. Chem.* **2007**, *15*, 2322.

[4] N. Coşkun, A. Öztürk, *Tetrahedron* **2007**, *63*, 1402.

[5] J. Zhu, B. M. Lines, M. D. Ganton, M. A. Kerr, M. S. Workentin, *J. Org. Chem.* **2008**, *73*, 1099.

[6] S. K. Hota, A. Chatterjee, P. K. Bhattacharya, P. Chattopadhyay, *Green Chem.* **2009**, *11*, 169.

[7] H. Özkan, Y. Yildirir, *J. Heterocycl. Chem.* **2010**, *47*, 954.

[8] A. P. Molchanova, P. S. Sorokoumova, J. Kopf, R. R. Kostikova, *Russ. J. Org. Chem.* **2011**, *47*, 66.

[9] A. R. Reddy, Z. Guo, F. M. Siu, C. N. Lok, F. Liu, K. C. Yeung, C. Y. Zhou, C. M. Che, *Org. Biomol. Chem.* **2012**, *10*, 9165.

[10] R. Badru, P. Anand, B. Singh, *Eur. J. Med. Chem.* **2012**, *48*, 81.

[11] P. Anand, B. Singh, *Bioorg. Med. Chem.* **2012**, *20*, 521.

[12] A. Kaur, B. Singh, A. S. Jaggi, *Bioorg. Med. Chem. Lett.* **2013**, *23*, 797.

[13] A. Kaur, B. Singh, *J. Heterocycl. Chem.* **2014**, *51*, 1421.

[14] H. Hou, S. Zhu, F. Pan, M. Rueping, *Org. Lett.* **2014**, *16*, 2872.

[15] G. R. Delpierre, M. Lamchen, *Q. Rev., Chem. Soc.* **1965**, *19*, 329.

[16] R. Jasinski, *Tetrahedron* **2013**, *69*, 927.

[17] R. Jasinski, *Tetrahedron Lett.* **2015**, *56*, 532.

[18] I. A. O'Neil, V. E. Ramos, G. L. Ellis, E. Cleator, A. P. Chorlton, D. J. Tapolczay, S. B. Kalindjian, *Tetrahedron Lett.* **2004**, *45*, 3659.

[19] M. Bakthadoss, A. Devaraj, *Tetrahedron Lett.* **2015**, *56*, 3954.

[20] E. Beccalli, G. Broggini, A. Contini, I. De Marchi, G. Zecchi, C. Zoni, *Tetrahedron: Asymmetry* **2004**, *15*, 3181.

[21] P. K. Biswas, D. Bandyopadhyay, T. Prange, A. Neuman, A. Banerji, *Synth. Commun.* **2011**, *41*, 1146.

[22] S. Minakata, T. Ezoe, K. Nakamura, I. Ryu, M. Komatsu, *Tetrahedron Lett.* **1998**, *39*, 5205.

[23] C. M. Braun, E. A. Congdon, K. A. Nolin, *J. Org. Chem.* **2015**, *80*, 1979.

[24] Q. Zhao, F. Han, D. L. Romero, *J. Org. Chem.* **2002**, *67*, 3317.

[25] R. Majer, O. Konechnaya, I. Delso, T. Tejero, O. A. Attanasi, S. Santeusanio, P. Merino, *Org. Biomol. Chem.* **2014**, *12*, 8888.

[26] W. Benchouk, S. M. Mekelleche, *RSC Adv.* **2015**, *5*, 22126.

[27] M. Cakici, S. Karabuga, H. Kilic, S. Ulukanli, E. Sahin, F. Sevin, *J. Org. Chem.* **2009**, *74*, 9452.

[28] R. A. Bawa, F. M. Gautier, H. Adams, A. J. H. M. Meijer, S. Jones, *Org. Biomol. Chem.* **2015**, *13*, 10569.

[29] S. Agopcan, N. Ç. Ölçüm, M. N. Üçışık, A. Sanyal, V. Aviyente, *Org. Biomol. Chem.* **2011**, *9*, 8079.

[30] S. A. Ali, M. Z. N. Iman, *Tetrahedron* **2007**, *63*, 9134.

[31] D. P. Curran, S. M. Choi, S. A. Gothe, F. T. Lin, *J. Org. Chem.* **1990**, *55*, 3710.

[32] P. Conti, G. Roda, H. Stabile, M. A. Vanoni, B. Curti, M. De Amici, *Farmaco* **2003**, *58*, 683.

[33] K. H. Park, M. J. Kurth, *J. Org. Chem.* **2000**, *65*, 3520.

[34] O. Kamm, *Org. Synth.* **1925**, *4*, 57.

[35] J. A. Passo, A. A. Merlo, J. Eccher, I. H. Bechtold, S. M. Kelly, *Quim. Nova* **2012**, *35*, 1527.

[36] I. Brüning, R. Grashey, H. Hauck, R. Huisgen, H. Seidl, *Org. Synth.* **1966**, *46*, 127.

[37] T. Oishi, M. Fujimoto, *J. Polym. Sci., Part A: Polym. Chem.* **1992**, *30*, 1821.

[38] M. P. Cava, A. A. Deana, K. Muth, M. J. Mitchell, *Org. Synth.* **1973**, *5*, 944.

[39] K. Aouadi, S. Vidal, M. Msaddek, J. P. Praly, *Synlett* **2006**, 3299.

[40] J. W. Sadownik, D. Philip, *Org. Biomol. Chem.* **2015**, *13*, 10392.

[41] F. E. Held, D. Grau, S. B. Tsogoeva, *Molecules* **2015**, *20*, 16103.

[42] D. Parmar, E. Sugiono, S. Raja, M. Rueping, *Chem. Rev.* **2014**, *114*, 9047.

[43] F. Heaney, O. Rooney, D. Cunningham, P. McArdle, *J. Chem. Soc., Perkin Trans.* **2001**, *2*, 373.

[44] D. Ginsburg, *Tetrahedron* **1983**, *39*, 2095.

[45] R. Jasinski, M. Ziolkowska, O. M. Demchuk, A. Maziarka, *Cent. Eur. J. Chem.* **2014**, *12*, 586.

[46] M. Ihara, M. Takahashi, K. Fukumoto, T. Kametani, *J. Chem. Soc., Chem. Commun.* **1988**, 9.

[47] T. Kametani, S. D. Chu, T. Honda, *J. Chem. Soc., Perkin Trans. 1* **1988**, 1593.

[48] M. Noguchi, H. Okada, S. Nishimura, Y. Yamagata, S. Takamura, M. Tanaka, A. Kakehi, H. Yamamoto, *J. Chem. Soc., Perkin Trans. 1* **1999**, (2), 185.

[49] L. Jaroskova, M. Konopikova, L. Fisera, *Chem. Papers* **1994**, *48*, 35.

[50] F. M. Cordero, S. Bonollo, F. Machetti, A. Brandi, *Eur. J. Org. Chem.* **2006**, 3235.

[51] D. R. López, T. Tejero, P. Merino, *J. Org. Chem.* **2014**, *79*, 8358.

[52] J. Hamer, A. Macaluso, *Chem. Rev.* **1964**, *64*, 473.

[53] A. D. Becke, *J. Chem. Phys.* **1993**, *98*, 5648.

[54] M. J. Frisch, G. W. Trucks, H. B. Schlegel, G. E. Scuseria, M. A. Robb, J. R. Cheeseman, J. A. Montgomery, Jr., T. Vreven, K. N. Kudin, J. C. Burant, J. M. Millam, S. S. Iyengar, J. Tomasi, V. Barone, B. Mennucci, M. Cossi, G. Scalmani, N. Rega, G. A. Petersson, H. Nakatsuji, M. Hada, M. Ehara, K. Toyota, R. Fukuda, J. Hasegawa, M. Ishida, T. Nakajima, Y. Honda, O. Kitao, H. Nakai, M. Klene, X. Li, J. E. Knox, H. P. Hratchian, J. B. Cross, V. Bakken, C. Adamo, J. Jaramillo, R. Gomperts, R. E. Stratmann, O. Yazyev, A. J. Austin, R. Cammi, C. Pomelli, J. W. Ochterski, P. Y. Ayala, K. Morokuma, G. A. Voth, P. Salvador, J. J. Dannenberg, V. G. Zakrzewski, S. Dapprich, A. D. Daniels, M. C. Strain, O. Farkas, D. K. Malick, A. D. Rabuck, K. Raghavachari, J. B. Foresman, J. V. Ortiz, Q. Cui, A. G. Baboul, S. Clifford, J. Cioslowski, B. B. Stefanov, G. Liu, A. Liashenko, P. Piskorz, I. Komaromi, R. L. Martin, D. J. Fox, T. Keith, M. A. Al-Laham, C. Y. Peng, A. Nanayakkara, M. Challacombe, P. M. W. Gill, B. Johnson, W. Chen, M. W. Wong, C. Gonzalez, J. A. Pople, *Gaussian 03, Revision E.01*, Gaussian, Inc., Wallingford, CT **2004**.

[55] M. Cossi, N. Rega, G. Scalmani, V. Barone, *J. Comput. Chem.* **2003**, *24*, 669.

[56] S. Grimme, J. Antony, S. Ehrlich, H. Krieg, *J. Phys. Chem.* **2010**, *132*, 154104.

[57] G. D. Tang, J. Y. Zhao, R. Q. Li, Y. Cao, Z. C. Zhang, *Spectrochim. Acta A* **2011**, *78*, 449.

[58] R. G. Parr, L. V. Szentpály, S. Liu, *J. Am. Chem. Soc.* **1999**, *121*, 1922.

[59] E. P. Elamurugu, S. Muthu, *Spectrochim. Acta A* **2015**, *134*, 453.

[60] T. A. Yousef, O. A. El-Gammal, S. F. Ahmed, G. M. Abu El-Reash, *Spectrochim. Acta A* **2015**, *135*, 690.

[61] R. R. Ternavisk, A. J. Camargo, F. B. C. Machado, J. A. F. F. Rocco, G. L. B. Aquino, V. H. C. Silva, H. B. Napolitano, *J. Mol. Model.* **2014**, *20*, 2526.

[62] M. Yavuz, H. Tanak, *J. Mol. Struct.: THEOCHEM* **2010**, *961*, 9.

[63] S. Y. Ebrahimipour, M. Abaszadeh, J. Castro, M. Seifi, *Polyhedron* **2014**, *79*, 138.

[64] E. R. Johnson, I. D. Mackie, G. A. DiLabio, *J. Phys. Org. Chem.* **2009**, *22*, 1127.

[65] S. Grimme, *Comput. Mol. Sci.* **2011**, *1*, 211.

[66] S. Grimme, *J. Comput. Chem.* **2004**, *25*, 1463.

[67] S. Grimme, *J. Comput. Chem.* **2006**, *27*, 1787.

[68] R. Jasinski, O. I. Koifman, A. Baranski, *Mendeleev Commun.* **2011**, *21*, 262.

[69] L. R. Domingo, M. J. Aurell, M. Arnó, J. A. Sáez, *J. Mol. Struct.: THEOCHEM* **2007**, *811*, 125.

[70] L. R. Domingo, *RSC Adv.* **2014**, *4*, 32415.

SUPPORTING INFORMATION

Additional Supporting Information may be found online in the supporting information tab for this article.

How to cite this article: Yıldırım, A., and Kaya, Y. (2016), High diastereoselectivity induced by intermolecular hydrogen bonding in [3 + 2] cycloaddition reaction: experimental and computational mechanistic approaches, *J. Phys. Org. Chem.*, doi: 10.1002/poc.3629